Computation of phase transformation dynamics in shape memory alloys based on a Landau-Ginzburg free energy model

Mahapatra, D.R. and Melnik, R.V.N.

In: Proceedings of the II ECCOMAS Thematic Conference on Smart Structures and Materials, Eds. Mota Soares C.A. et al, Lisbon, 15 pages, 2005.

II ECCOMAS Thematic Conference on Smart Structures and Materials

Paper

Design by: Ana Espada & Leonardo Rosado :: lhr@netcabo.pt

Instituto Superior Técnico, Lisbon 18 / 21 July 2005

FUNDAÇÃO CALOUSTE GULBENKIAN

FCT Fundação para a Ciência e a Tecnologia
MINISTÉRIO DA CIÊNCIA, TECNOLOGIA E ENSINO SUPERIOR

APMTAC

II ECCOMAS THEMATIC CONFERENCE ON SMART STRUCTURES AND MATERIALS
C.A. Mota Soares *et al.* (Eds.)
Lisbon, Portugal, July 18 - 21, 2005

COMPUTATION OF PHASE TRANSFORMATION DYNAMICS IN SHAPE MEMORY ALLOYS BASED ON A LANDAU-GINZBURG FREE ENERGY MODEL

D. Roy Mahapatra* **and Roderick V.N. Melnik†**

* Mathematical Modelling and Computational Sciences, Wilfrid Laurier University
75 University Avenue West, Waterloo, ON, N2L3C5, Canada
e-mail: rmelnik@wlu.ca

† Mathematical Modelling and Computational Sciences, Wilfrid Laurier University
75 University Avenue West, Waterloo, ON, N2L3C5, Canada
e-mail: droymahapatra@wlu.ca

Keywords: Shape Memory Alloy, Phase Transformation, Multivariant, Thermoelastic, Finite Element.

Abstract. *Landau theory has been successfully applied to the solution of dynamic problems of martensitic phase transformations in alloys. On the other hand, precise mathematical description of the microstructures is known within the framework of Cauchy-Born hypothesis, although the discrete version of this description is not well elucidated for multivariant transformations in three-dimensional samples because of various computational difficulties while handling a quasi-convex minimization problem. In this paper, we develop a new Landau-Ginzburg free energy model for such a problem and demonstrate its link with the continuum description of phase transformations. This leads us to a possiblity of using the precise description of compatible microstructures in the phase-field model that allows us to improve computational effectiveness of the finite element model. The proposed formulation is general and can be applied to different types of phase transforming alloys under different thermo-mechanical loadings. Numerical results for cubic to tetragonal transformations are reported.*

1 INTRODUCTION

Shape Memory Alloys (SMAs) are known to have various proven applications in transducer devices and in control of dynamical systems. However, the design and analysis of new SMA structures remain extremely difficult and numerous phenomenological models have been reported in the literature to simplify these processes. Such phenomenological models vary drastically depending on material constants, conditions at which experiments are done, effective dimension and size of the sample and the nature of thermo-mechanical loading. Thus, over the past few decades researchers have been seeking a deeper mathematical understanding of

the origin of the SMA microstructure under deformation (see e.g. [1, 2, 3, 4, 5, 6, 7]), while computational challenges encountered in the applications of the related theories have recently been reviewed in [8]. It has been pointed out that the sequence of minimization processes over a set of austenite-martensite energy wells gives rise to the observed microstructure having precise analytical description [1, 9]. At the macroscopic scale, these local deformations, which are equivalent to transformation of Austenite (A) to Martensitic variants (M) and the reverse transformation, give rise to the shape-memory effect. Although the effect has known for a long time, not much developments have taken place till date in which the three-dimensional and time-dependent dynamics of real-scale SMA devices have been studied by linking this theoretical framework to practical engineering applications. The main difficulties encountered in achieving this numerically lie with the underlying interdependence of the following two aspects: (1) the sequence of energy density minimization (at the end of which the global minimum may not be actually attained under the prescribed dynamic loading and prescribed macroscopic constraints; the discrete version of the process is referred to as quasi-convexification of the original non-convex minimization problem), and (2) the conditions required to match the spatial discretization with the evolved interfaces dynamically (meaning that an efficient implementation of a mesh adaptation scheme within the variational framework, e.g. adaptive finite elements, is usually required).

In the present paper, we propose a new model based on the Landau-Ginzburg theory in the context of first-order phase-field evolution applicable to SMAs (see [10, 11, 12, 13]) and discuss its link with the microstructural compatibility under the framework of macroscopic continuum deformation (for details see [9]). A major advantage of the proposed approach is that the requirement of mesh adaptation scheme mentioned above in (2) is relaxed when we interpolate the phase field itself (represented by order parameter η). However, consistent evolution criteria need to be derived from the analytic description of the microstructure using the compatibility conditions. In this paper, we outline the possible steps to achieve this. Among other major issues, we mention the problem of the description of the energy wells $G(\eta)$ in case of multivariant Phase Transformation (PT) with essential properties of frame-indifference and material symmetry. Further conditions are to be imposed regarding the uniqueness of the evolution, in particular that only a single variant is formed at a given point in space and time. Details of a systematic approach to impose these conditions can be found in [14, 15]. Recall further that the evolution of the ordered states, or equivalently the A-M compatible microstructure, is governed by a first-order kinetics, known as the time-dependent Ginzburg-Landau equation [4, 13]. However, in order to complete the description of the model, the value of the spontaneous strains and certain material parameters are to be estimated from a molecular dynamic simulation. This was done in [15] by assuming time-independent and thermo-elastically decoupled case. The underlying step here is to obtain, on the one hand, the atomistic reordering without diffusion and the resulting free energy $G(\eta)$ (or the related constants and spontaneous strain at equilibrium temperature) based on the Born-Oppenheimer approximation, and on the other hand, express this free energy (equivalently $G(F)$) according to the Cauchy-Born hypothesis. The order parameters (η_k), therefore, describe the phenomenological link between the above two dynamics. This

approach deviates from the notion of phase fractions [16, 17] and gives a consistent framework for microstructure evolution in multivariant situations.

Given the problem complexity, it does not come as a surprise that till date there is no robust mathematical model and well-defined computational steps that can deal with general time-dependent dynamics of SMA over a range of deformation, stress and temperature. Nevertheless, rigorous analytical statements on the stability and bounds of the numerical solutions of energy minimization have been drawn (e.g. Li and Luskin [18], Matus *et al.* [19]).

The organization of the paper is as follows. In Sec. 2 we outline the steps to derive $G(\eta)$. Extension of this representation to the three-dimensional multivariant case is given in Sec. 3. The link between the phase-field evolution and the microstructural compatibility condition is drawn in Sec. 3.1. The behaviour of the energy wells under thermoelastic deformation is numerically analyzed in Sec. 3.2. Finite element formulation involving the quasi-convex minimization of energy functional at a given step is reported in Sec. 3.3. Simulations of stress induced transformation dynamics are presented in Sec. 5

2 LANDAU-GINZBURG FREE ENERGY MODEL FOR MULTIVARIANT MARTENSITIC TRANSFORMATION

It has been demonstrated by Levitas and Preston [14, 4] that the polynomial structures 2-3-4 and 2-4-6 of the Gibbs free energy in order parameter η in Cartesian coordinate can eliminate the problem of unphysical minima and retain all the necessary properties of the Ginzburg-Landau free energy function with respect to point group symmetry of the crystals. Also such polynomial structure can be made in such a way that the stability of the austenitic phase (A) and martensitic variants (M_j), non-minimum diffusion barrier and nucleation can be described in stress-temperature space. Also, while using such a polynomial structure, the interfaces (domain walls) $M_j - M_i$ between the martensitic variants (i, j) can be interpreted by using a newly introduced barrierless A nucleation mechanism, i.e. by splitting the original into two simultaneously present interfaces $M_j - A$ and $A - M_i$. In this section a 2-3-4 polynomial structure is constructed by improving upon the model of Levitas and Preston [14, 15]. Below we briefly describe the Gibbs free energy representation for our model. The details are given in [20].

Let us first consider a single variant of martensite and single order parameter $\eta \in [0, 1]$. First we define the Gibbs free energy density in stress-temperature space $(\boldsymbol{\sigma}, \theta)$ as

$$G(\eta) = -\boldsymbol{\sigma} : \boldsymbol{\lambda} : \boldsymbol{\sigma}/2 - \boldsymbol{\sigma} : \boldsymbol{\varepsilon}_t \varphi(\eta) + f(\theta, \eta) \ , \tag{1}$$

where $\boldsymbol{\lambda}$ is the constant fourth-rank elastic compliance tensor, $\boldsymbol{\varepsilon}_t$ is the transformation strain tensor at the thermodynamic equilibrium of the martensite (obtained from crystallography), $\varphi(\eta)$ is a monotonic function with $\varphi(0) = 0$ indicating stable A phase and $\varphi(1) = 1$ indicating stable M phase. $f(\theta, \eta)$ is the chemical part of the energy with property: $f(\theta, 1) - f(\theta, 0) = \Delta G^{\theta}(\theta)$, where ΔG^{θ} is the difference between the thermal parts of the Gibbs free energy density of the M and A phases, which can be obtained indirectly from experiments through the relation [21]

$$\Delta G^{\theta} = -\Delta s_e(\theta - \theta_e) - \Delta c\theta \left[\ln(\theta/\theta_e) - 1\right] - \Delta c\theta_e \ , \tag{2}$$

where Δc is the difference between the specific heat of the phases, Δs_e is the jump in the specific entropy at the equilibrium temperature (θ_e). The objective is to obtain the functions φ and f by satisfying their properties mentioned above and the conditions of extremum of the energy for existence of equilibrium of A and M phases: $\partial G/\partial \eta = 0$ at $\eta = 0, 1$. Thus main step in the subsequent formulation that follows [20] is to assume the extremum in the form

$$\frac{\partial G}{\partial \eta} = \eta(\eta - 1)(\eta - \eta_b) \ , \tag{3}$$

so that the roots $\eta = 0, 1$ correspond to the extrema and the root $\eta = \eta_b(\boldsymbol{\sigma}, \theta)$ represents the $A \leftrightarrow M$ PT barrier. Integrating Eq. (3) and imposing the combined properties of $\varphi(\eta)$ and $f(\theta, \eta)$ stated earlier as

$$G(\boldsymbol{\sigma}, \theta, 0) - G(\boldsymbol{\sigma}, \theta, 1) = \boldsymbol{\sigma} : \boldsymbol{\varepsilon}_t - \Delta G^{\theta} \ , \tag{4}$$

we get

$$\eta_b = -6\boldsymbol{\sigma} : \boldsymbol{\varepsilon}_t + 6\Delta G^{\theta} + 1/2 \ . \tag{5}$$

After some algebraic steps, we explicitely obtain the polynomial structure in $\varphi(\eta)$ and then $f(\theta, \eta)$. For $A \rightarrow M$ PT, the criteria for the loss of stability of A phase is $\partial^2 G/\partial \eta^2 \leq 0$ at $\eta = 0$. Similarly, for $M \rightarrow A$ PT, the criteria for the loss of stability is $\partial^2 G/\partial \eta^2 \leq 0$ at $\eta = 1$. This procedure is extended to the multivariant case in the next section.

3 MULTIVARIANT PHASE TRANSFORMATION

In order to model realistic situations and macroscopic sample of SMA, it is essential to incorporate the effects of the following: (1) martensitic variants (M_k), (2) thermal strain, (3) unequal compliances across the interfaces and the resulting inhomogeneity. In this paper we consider cubic-to-tetragonal transformations for numerical studies. In this case, there are three variants of martensite according to the point group of crystallographic symmetry. The Gibbs free energy density thus should possess the associated invariance properties. In the mathematical model, this can be cross-checked by interchanging the variant indices (k). We assume the same order of variation in the compliance tensor and the thermal expansion tensor as in $\varphi(\eta)$. The Gibbs free energy density for cubic-tetragonal transformation having three variants $k = 1, 2, 3$ is expressed as

$$\begin{aligned} G(\eta) = -\boldsymbol{\sigma} : \left[\boldsymbol{\lambda}_0 + \sum_{k=1}^{3} (\boldsymbol{\lambda}_k - \boldsymbol{\lambda}_0)\varphi(\eta_k) \right] : \boldsymbol{\sigma}/2 - \boldsymbol{\sigma} : \sum_{k=1}^{3} \boldsymbol{\varepsilon}_{tk}\varphi(\eta_k) \\ -\boldsymbol{\sigma} : \left[\boldsymbol{\varepsilon}_{\theta 0} + \sum_{k=1}^{3} (\boldsymbol{\varepsilon}_{\theta k} - \boldsymbol{\varepsilon}_{\theta 0})\varphi(\eta_k) \right] + \sum_{k=1}^{3} f(\theta, \eta_k) + \sum_{i=1}^{2} \sum_{j=i+1}^{3} F_{ij}(\eta_i, \eta_j) \ , \end{aligned} \tag{6}$$

where $\boldsymbol{\lambda}$ is the second-order forth-rank compliance tensor ($\boldsymbol{\lambda}_0$ is for A phase), $\boldsymbol{\varepsilon}_{\theta 0} = \boldsymbol{\alpha}_0(\theta - \theta_e)$, $\boldsymbol{\varepsilon}_{\theta k} = \boldsymbol{\alpha}_k(\theta - \theta_e)$, $\boldsymbol{\alpha}_0$ and $\boldsymbol{\alpha}_k$ are the thermal expansion tensor of A and M_k. F_{ij} is an interaction potential required to preserve the frame-invariance of G with respect to the point group of symmetry and uniqueness of the multivariant PT at a given material point. The description

of PT can now be generalized with three sets of order parameters: $\bar{0} = \{0, \eta_k = 0, 0\}$, $\bar{1} = \{0, \eta_k = 1, 0\}$ and $\bar{\eta}_k = \{0, \eta_k, 0\}$. The extremum property of the free energy density requires

$$\frac{\partial G}{\partial \eta_k} = \eta_k(\eta_k - 1)(\eta_k - \eta_{bk}) = 0 \ , \quad \eta_k = \bar{0}, \bar{1} \ , \tag{7}$$

$$\frac{\partial^2 G}{\partial \eta_k^2} \leq 0 \ , \quad \eta_k = \bar{0} \quad (A \rightarrow M_k) \tag{8}$$

$$\frac{\partial^2 G}{\partial \eta_k^2} \leq 0 \ , \quad \eta_k = \bar{1} \quad (M_k \rightarrow A) \tag{9}$$

The transformation energy associated with $A \leftrightarrow M_k$ is

$$G(\boldsymbol{\sigma}, \theta, \bar{0}) - G(\boldsymbol{\sigma}, \theta, \bar{1}) = \boldsymbol{\sigma} : \boldsymbol{\varepsilon}_{tk} - \Delta G^{\theta} \ . \tag{10}$$

Combining Eqs. (7) and (10) with similar steps described in Sec. 2 and discussed in detail in [20], we get

$$\eta_{bk} = -6\boldsymbol{\sigma} : \boldsymbol{\varepsilon}_{tk} - 6\boldsymbol{\sigma} : (\boldsymbol{\lambda}_k - \boldsymbol{\lambda}_0) : \boldsymbol{\sigma}/2 - 6\boldsymbol{\sigma} : (\boldsymbol{\varepsilon}_{\theta k} - \boldsymbol{\varepsilon}_{\theta 0}) + 6\Delta G^{\theta} + 1/2 \tag{11}$$

Following the steps given in [15], we arrive at the frame-invariance as well as symmetry preserving polynomial structure of the interaction potential

$$F_{ij} = \eta_i \eta_j (1 - \eta_i - \eta_j) \left[B \left\{ (\eta_i - \eta_j)^2 - \eta_i - \eta_j \right\} + D\eta_i \eta_j \right] + \eta_i^2 \eta_j^2 (\eta_i Z_{ij} + \eta_j Z_{ji}) \tag{12}$$

where B, D are constants to be estimated from experiments, The transformation energy associated with $M_i \rightarrow M_j$ is already satisfied in this approach. Finally, the uniqueness of multi-variant PT at a material point is now imposed, which leads to

$$\frac{\partial}{\partial \boldsymbol{\sigma}} \left[\sum_{k=1}^{2} \sum_{j=k+1}^{3} \frac{\partial F_{kj}(\eta_k, \eta_j)}{\partial \eta_k} \right] = \sum_{k=1}^{3} \left[\boldsymbol{\varepsilon}_{tk} \frac{\partial \varphi(\eta_k)}{\partial \eta_k} + (\boldsymbol{\varepsilon}_{\theta k} - \boldsymbol{\varepsilon}_{\theta 0}) \frac{\partial \varphi(\eta_k)}{\partial \eta_k} \right.$$
$$\left. + (\boldsymbol{\lambda}_k - \boldsymbol{\lambda}_0) \frac{\partial \varphi(\eta_k)}{\partial \eta_k} \boldsymbol{\sigma} \right] \ , \tag{13}$$

The constants Z_{ij} can be estimated with the help of Eq. (13).

It can be noted that the energy density is represented in stress-temperature space. In this way the direct use of the deformation gradient associated with the phase transformation is avoided. As a consequence, analysis in stress space without explicitely addressing the stress-strain hysteresis becomes convenient (see [15]). On the other hand, if the atomic reordering during transformation is expressed in terms of continuum deformation gradient $\boldsymbol{F} = \nabla \boldsymbol{y}(\boldsymbol{x})$, then the associated large strain for the two equivalent models can be given by

$$\frac{1}{2} \left(\boldsymbol{F}^T \boldsymbol{F} - \boldsymbol{I} \right) = -\frac{\partial G(\eta)}{\partial \boldsymbol{\sigma}} = \boldsymbol{\varepsilon}_{\mathrm{elt}} + \sum_k \boldsymbol{\varepsilon}_{tk} \varphi(\eta_k) \ , \tag{14}$$

where $\boldsymbol{\varepsilon}_{\mathrm{elt}}$ is the elastic part of the total strain from Eq. (6). For a compatible microstructure that minimizes $G(\boldsymbol{F}) \in \mathcal{K}$ at the austenitic well, where $\mathcal{K}$ is the sequence of energy wells, it

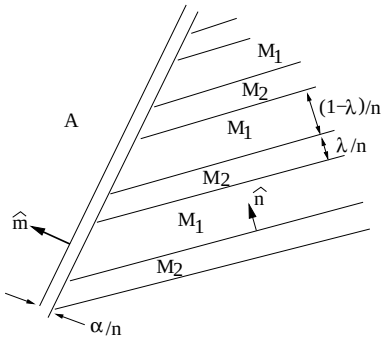

Figure 1. Alternate array of microstructure originating from austenite wall.

follows from the Cauchy-Born hypothesis that

$$\hat{\mathbf{e}}^m = \boldsymbol{F}^m \boldsymbol{U}_m \boldsymbol{F}^a \hat{\mathbf{e}}^o \ , \tag{15}$$

where $\hat{\mathbf{e}}^m$ and $\hat{\mathbf{e}}^o$ are the lattice vectors for the mth variant of M and the undeformed A lattice vector respectively. Under zero stress, $\boldsymbol{F}^m = \boldsymbol{F}^a = \boldsymbol{R}$ is a rigid rotation. $\boldsymbol{U}_m$ is the Bain matrix or the transformation matrix [9]. At the onset of spontaneous transformation, we can drop the elastic strain part in Eq. (15) such that

$$\frac{1}{2}\left(\boldsymbol{U}_m^T \boldsymbol{U}_m - \boldsymbol{I}\right) = \sum_k \varepsilon_{tk} \varphi(\eta_k) \ . \tag{16}$$

Left hand side of Eq.(16) is a point-wise description, whereas the right hand side requires a spatial structure $\eta_k \in \{\eta_k(\boldsymbol{x})\}$. Interestingly, this spatial description is already present in $\boldsymbol{F}(\boldsymbol{x})$ and has close-form solution following the works of Ball [1] and the references therein for rank-one connected phases under plane strain condition. For 3D situations with more complex interfaces, the solution can be sought numerically. A general approach that can be adopted in introducing such microstructural compatibility in the phase-field is described below.

3.1 Compatible microstructure

Let us consider the alternate array like microstructure shown in Fig. 1 often observed in micrographs of SMA where λ is the alternate M width. The average deformation gradients in A, M_k are respectively $\boldsymbol{F}^{(o)}$, $\boldsymbol{F}^{(k)}$. For given transformation matrices $\boldsymbol{U}_k$, let λ_1, λ_2, λ_3 be the eigenvalues of $\boldsymbol{U}_k$. For the average deformation across the M_1-M_2 interfaces to be compatible (for detail derivation see [9])

$$\boldsymbol{F}^{(2)} - \boldsymbol{F}^{(1)} = \boldsymbol{a}' \otimes \hat{\mathbf{n}} \ . \tag{17}$$

This is called the twinning equation. For the A-M_k be formed as n increases but for an interface to exist with continuous deformation,

$$\lambda \boldsymbol{F}^{(2)} + (1-\lambda)\boldsymbol{F}^{(1)} - \boldsymbol{F}^{(o)} = \boldsymbol{b} \otimes \hat{\mathbf{m}} \ . \tag{18}$$

a' and b are some scalars to be identified. This is called the A-M interface equation. Using the invariance properties, i.e.,

$$\boldsymbol{F}^{(o)} = \boldsymbol{I} \ , \quad \boldsymbol{F}^{(1)} = \boldsymbol{Q}_1\boldsymbol{U}_1 \ , \quad \boldsymbol{F}^{(2)} = \boldsymbol{Q}_2\boldsymbol{U}_2 \tag{19}$$

and so on for all the variants, where $\boldsymbol{Q}$ is some rotation matrix, one finds

$$\boldsymbol{b} = \rho' \left(\sqrt{\frac{\lambda_3(1-\lambda_1)}{\lambda_3-\lambda_1}}\hat{\mathbf{e}}_1 \pm \sqrt{\frac{\lambda_1(\lambda_3-1)}{\lambda_3-\lambda_1}}\hat{\mathbf{e}}_2 \right) \ , \tag{20}$$

$$\hat{\mathbf{m}} = \frac{\sqrt{\lambda_3}-\sqrt{\lambda_1}}{\rho'\sqrt{\lambda_3-\lambda_1}} \left(-\sqrt{1-\lambda_1}\hat{\mathbf{e}}_1 \pm \sqrt{\lambda_3-1}\hat{\mathbf{e}}_2 \right) \ , \tag{21}$$

with $\lambda_1 \leq \lambda_2 \leq \lambda_3$ as three eigen values of $\boldsymbol{U}_k$, $\lambda_2 = 1$, and ρ' is such that $|\hat{\mathbf{m}}| = 1$.

For given $\boldsymbol{Q}_k$ and $\hat{\mathbf{n}}$ (the orientation of the domain walls), $\boldsymbol{F}^{(k)}$ can be solved using Eqs. (17) and (18). It is then reasonable to decompose Eq. (16) the variant-wise contribution of strain as

$$\frac{1}{2}\left(\boldsymbol{F}_k^T\boldsymbol{F}_k - \boldsymbol{I}\right) = \boldsymbol{\varepsilon}_{tk}\varphi(\eta_k) \ . \tag{22}$$

η_k can be obtained from Eq. (22) as trial solution for microstructural evolution in the proposed phase-field model. In this paper the discrete version of the minimization problem is developed based on a finite element model with $\eta_k(\boldsymbol{x})$ as additional interpolation variable.

3.2 Energy wells under thermomechanical loading

For numerical illustration of the Gibbs free energy function derived in Sec.3, we consider NiAl with two martensitic variants.

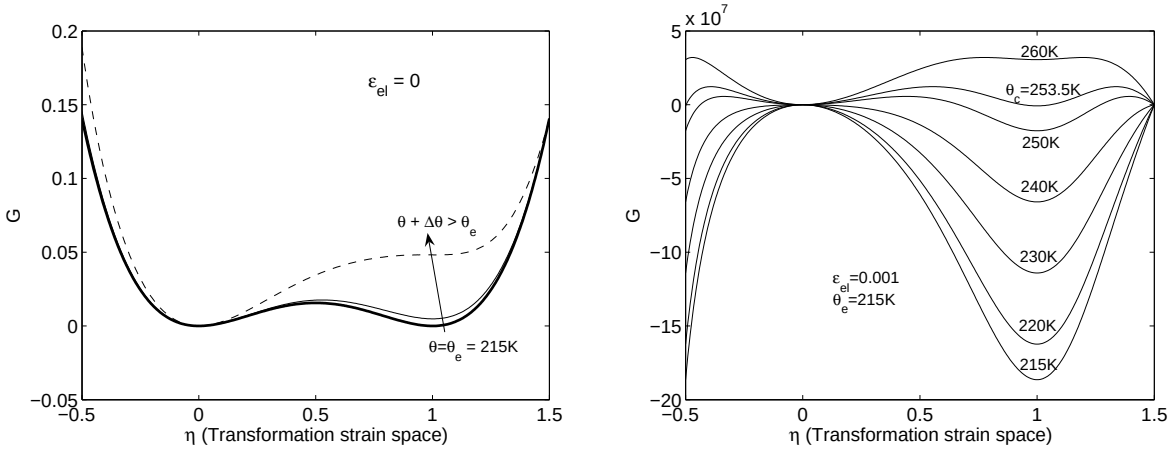

(a) (b)

Figure 2. (a) Austenitic well at temperature above critical temperature ($\theta_c = \theta_e$) under zero elastic deformation (b) Formation of martensitic wells at decreasing temperature and constant elastic deformation.

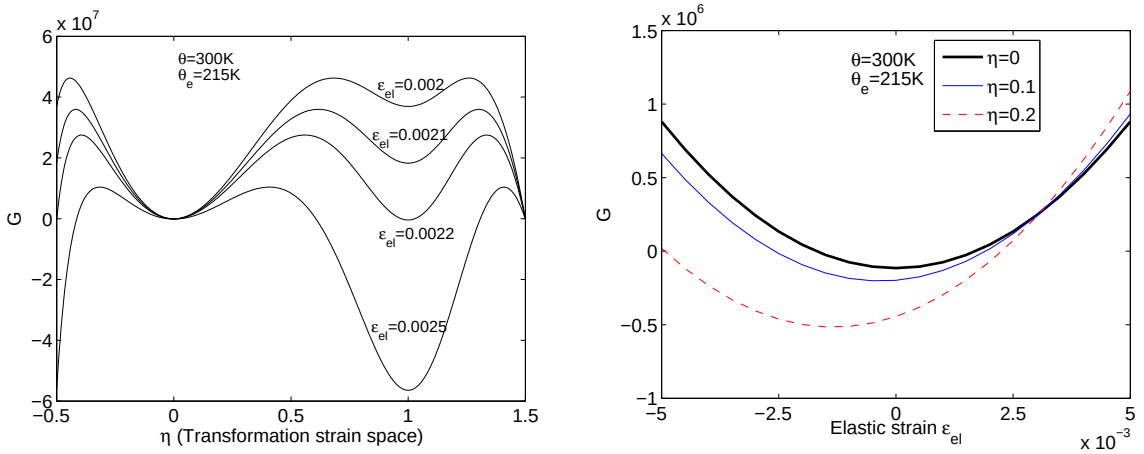

(a) (b)

Figure 3. (a) Formation of martensitic wells under increasing deformation and constant temperature (b) Inversion-symmetry preserving structure of the energy well during the evolution of η.

Equal deviations of critical temperature from equilibrium temperature are assumed. The internal energy is assumed to be proportional to the difference between temperature and the equilibrium temperature in the close neighborhood of the transformation [15]. Figs. 2(a)-(b) and 3(a) show the structure of the energy well, where the martensitic minimum can be formed at $\theta < \theta_c$ where θ_c is the critical temperature or at increasing deformation under controlled temperature. Fig. 3(b) shows that the inversion-symmetry of the energy well in strain space is preserved but the axis of symmetry shifts to lower elastic deformation when the martensitic phase is formed. Results for two variants of M in rank-1 connected system are shown in Figs. 4(a) and (b).

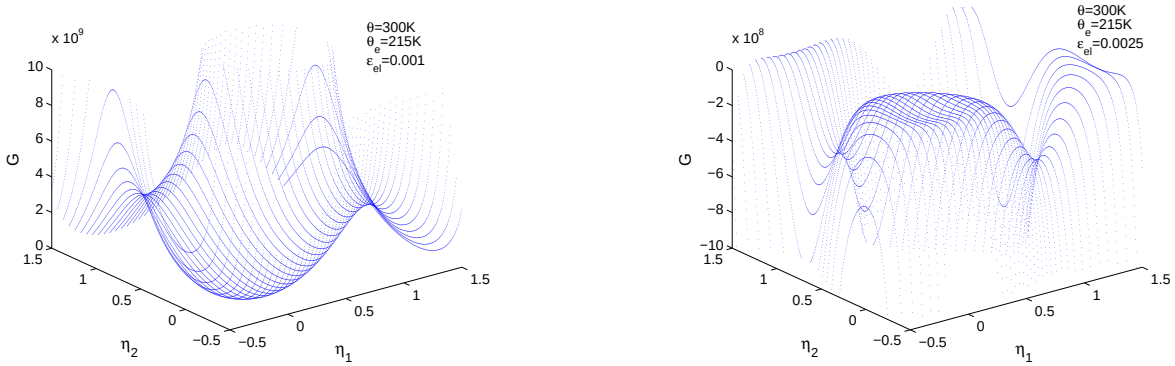

(a) (b)

Figure 4. (a) Unique minimum at the austenitic well ($\eta_1 = \eta_2 = 0$) under constant average deformation and temperature above the critical temperature (b) Unique martensitic wells ($\eta_1 = 1, \eta_2 = 0$) and ($\eta_1 = 0, \eta_2 = 1$) at temperature above the equilibrium temperature but under increased deformation.

It can be seen from Figs. 4(a) and (b) that the developed free energy model retains the symmetry, invariance and uniqueness properties while accommodating the combined effect of deformation and temperature.

3.3 VARIATIONAL FRAMEWORK FOR THE QUASI-CONVEX ENERGY MINIMIZATION PROBLEM

In the phase-field model, the transformation kinetics is governed by the Ginzburg-Landau equation

$$\frac{\partial \eta_k}{\partial t} = -\sum_{p=1}^{3} L_{kp}\left[\frac{\partial G}{\partial \eta_p} + \boldsymbol{\beta}_p : \boldsymbol{\nabla}\boldsymbol{\nabla}\eta_p\right] + \theta_k \ , \tag{23}$$

where L_{kp} are positive definite kinetic coefficients, $\boldsymbol{\beta}_p$ are positive definite second rank tensor. θ_k is the thermal fluctuation satisfying the dissipation-fluctuation theorem arising in context of non-equilibrium thermodynamics. While Eq. (23) governs the evolution process, the macroscopic energy conservation law is governed by the heat conduction equation

$$\rho\frac{\partial \bar{G}}{\partial t} - \boldsymbol{\sigma} : \boldsymbol{\nabla}\frac{\partial \boldsymbol{u}}{\partial t} + \boldsymbol{\nabla}.\boldsymbol{q} = h_\theta \ , \tag{24}$$

and the momentum balance equation

$$\rho\frac{\partial^2 \boldsymbol{u}}{\partial t^2} = \boldsymbol{\nabla}.\boldsymbol{\sigma} + \boldsymbol{p} \ , \tag{25}$$

where

$$\bar{G} = G - \theta\frac{\partial G}{\partial \theta} \tag{26}$$

is the internal energy, ρ is the mass density, $\boldsymbol{u}$ is the displacement vector,

$$\boldsymbol{q} = -\kappa\boldsymbol{\nabla}\theta - \alpha'\kappa\boldsymbol{\nabla}\frac{\partial \theta}{\partial t} \tag{27}$$

is the heat flux approximated from the solution of 3D Cattaneo-Vernotte equation [6], h_θ and $\boldsymbol{p}$ are the thermal loading and body force, respectively. In a quasi-static sense, the framework so far requires the minimization of the total energy[1, 22]

$$\int_\Omega G(\nabla \mathbf{u}(\mathbf{x}), \theta)\mathrm{d}\mathbf{x} + \text{loading device energy} \ , \tag{28}$$

expressed in the deformed configuration of the lattice. Thus, in our model, the order parameters η_k, which appears in the total strain and related to the macroscopic deformation as in Eq. (22), provides the important connection between the transformation of the lattice vector and the continuum deformation gradient. Further, in order to model the evolution process, one requires a variational formulation involving a suitable weak form of the Initial Boundary Value Problem (IBVP). This is discussed in the following section where we develop a three-dimensional finite element model of the IBVP.

3.4 Spatial discretization

We interpolate the fields $\boldsymbol{u}(x,y,z,t)$, $\theta(x,y,z,t)$ and $\eta_k(x,y,x,t)$ $(k=1,\cdots,n)$ using non-conforming finite element, with h-refinement. This is an established scheme for modeling SMA microstructure [18]. Noting that all the three governing equations have highest order of spatial derivative as two, we choose the standard Lagrangian isoparametric interpolation function $\boldsymbol{N}$,

$$\{u_1\ u_2\ u_3\}^T = \boldsymbol{N}_u \boldsymbol{v}^e\ , \quad \theta = \boldsymbol{N}_\theta \boldsymbol{v}^e\ , \quad \eta = \boldsymbol{N}_\eta \boldsymbol{v}^e\ , \tag{29}$$

$$\boldsymbol{v} = \{u_1\ u_2\ u_3\ \theta\ \eta_1\ ,\cdots,\eta_n\}^T\ . \tag{30}$$

Here, the superscript e indicates element nodal quantities. Introducing admissible weights $(\bar{u}_i, \bar{\theta}, \bar{\eta}_k)$ chosen from the linear span of $\boldsymbol{v}^e$, a variational statement can be posed as

$$\delta\Pi = \delta\Pi_{\rm PT} + \delta\Pi_\theta + \delta\Pi_u + \delta W = 0\ , \quad t\in[0,+\infty] \tag{31}$$

where

$$\Pi_{\rm PT} = \int_\Omega \sum_{k=1}^n \bar{\eta}_k \left[\frac{\partial \eta_k}{\partial t} - \theta_k\right] {\rm d}\mathbf{x} + \int_\Omega \sum_{k=1}^n \sum_{p=1}^n \eta_k \left[L_{kp}\left(\frac{\partial G}{\partial \eta_p} + \boldsymbol{\beta}_p : \boldsymbol{\nabla}\boldsymbol{\nabla}\eta_p\right)\right] {\rm d}\mathbf{x}\ , \tag{32}$$

$$\Pi_\theta = \int_\Omega \bar{\theta}\left[\rho\frac{\partial \bar{G}}{\partial t} - \boldsymbol{\sigma} : \boldsymbol{\nabla}\frac{\partial \boldsymbol{u}}{\partial t}\right] {\rm d}\mathbf{x} + \int_\Omega \theta\left[\boldsymbol{\nabla}.\left(-\kappa\boldsymbol{\nabla}\theta - \alpha'\kappa\boldsymbol{\nabla}\frac{\partial\theta}{\partial t}\right) - h_\theta\right] {\rm d}\mathbf{x}\ , \tag{33}$$

$$\Pi_u = \int_{t_1}^{t_2}\int_\Omega \bar{\boldsymbol{u}}\left[\rho\frac{\partial^2 \boldsymbol{u}}{\partial t^2} - \boldsymbol{\nabla}.\boldsymbol{\sigma} - \boldsymbol{p}\right] {\rm d}\mathbf{x}\ , \tag{34}$$

and W is the external work done. Integrating Eqs. (29)-(31) by parts and applying divergence theorem, we get the discrete nonlinear finite element model, which can be expressed in matrix notations as

$$\{\delta\boldsymbol{u}\}^e: \quad \int_\Omega [\boldsymbol{N}_u]^T\rho[\boldsymbol{N}_u]\{\ddot{\boldsymbol{v}}\}^e + \int_\Omega [\boldsymbol{B}_u]^T\{\boldsymbol{\sigma}\} = \int_\Gamma [\boldsymbol{N}_u]^T\{\boldsymbol{p}\} + \{\boldsymbol{f}\}^e\ , \tag{35}$$

$$\begin{aligned}\{\delta\theta\}^e: \quad & \int_\Omega [\boldsymbol{N}_\theta]^T\rho[\dot{\boldsymbol{G}}']\{\boldsymbol{v}\}^e + \int_\Omega [\boldsymbol{N}_\theta]^T\rho[\boldsymbol{G}']\{\dot{\boldsymbol{v}}\}^e \\ & - \int_\Omega [\boldsymbol{N}_\theta]^T\rho[\boldsymbol{N}_\theta]\{\boldsymbol{v}\}^e\left([\nabla_\theta\dot{\boldsymbol{G}}']\{\boldsymbol{v}\}^e + [\nabla_\theta\boldsymbol{G}']\{\dot{\boldsymbol{v}}\}^e\right) \\ & + \int_\Omega [\boldsymbol{N}_\theta]^T\{\boldsymbol{\sigma}\}^T[\nabla\boldsymbol{N}_u]\{\boldsymbol{v}\}^e + \int_\Omega [\boldsymbol{B}_\theta]^T\kappa[\boldsymbol{B}_\theta]\{\boldsymbol{v}\}^e \\ & + \int_\Omega [\boldsymbol{B}_\theta]^T\alpha'\kappa[\boldsymbol{B}_\theta]\{\dot{\boldsymbol{v}}\}^e = \int_\Gamma [\boldsymbol{N}_\theta]^T\{\boldsymbol{q}_\theta\}^e\ ,\end{aligned} \tag{36}$$

$$\begin{aligned}\{\delta\boldsymbol{\eta}\}: \quad & \int_\Omega [\boldsymbol{N}_\eta]^T[\boldsymbol{N}_\eta]\{\dot{\boldsymbol{v}}\}^e + \int_\Omega [\boldsymbol{N}_\eta]^T[\boldsymbol{L}][\boldsymbol{G}'']\{\boldsymbol{N}_\eta\}\{\boldsymbol{v}\}^e \\ & - \int_\Omega [\nabla\boldsymbol{N}_\eta]^T[\boldsymbol{L}][\boldsymbol{\beta}][\nabla\boldsymbol{N}_\eta]\{\boldsymbol{v}\}^e + \int_\Gamma [\boldsymbol{N}_\eta]^T[\boldsymbol{L}][\boldsymbol{\beta}][\nabla\boldsymbol{N}_\eta]\{\boldsymbol{v}\}^e = \int_\Gamma [\boldsymbol{N}_\eta]^T\{\theta_k\}^e\ ,\end{aligned}$$

where $[\boldsymbol{B}_u]$ is the strain-displacement matrix and $[\boldsymbol{B}_\theta]$ is its thermal analog. The stress vector is expressed as

$$\{\boldsymbol{\sigma}\} = [\boldsymbol{C}(\eta_k)][\boldsymbol{B}_u]\{\boldsymbol{v}\}^e - [\boldsymbol{C}^t(\eta_k, \boldsymbol{\varepsilon}_{tk})][\boldsymbol{N}_\eta]\{\boldsymbol{v}\}^e$$

$$-[\boldsymbol{C}^\alpha(\eta_k, \alpha_0, \alpha_k)][\boldsymbol{N}_\theta]\left(\{\boldsymbol{v}\}^e - [\boldsymbol{I}]\{\theta_e\}\right) \ , \tag{37}$$

where the elastic stiffness including the phase inhomogeneity

$$[\boldsymbol{C}(\eta_k)] = \left[[\boldsymbol{\lambda}_0] + \sum_k \left([\boldsymbol{\lambda}_k] - [\boldsymbol{\lambda}_0]\right)\varphi(\eta_k)\right]^{-1} \ , \tag{38}$$

the transformation-induced stress coefficient matrix

$$[\boldsymbol{C}^t(\eta_k, \boldsymbol{\varepsilon}_{tk})] = [\boldsymbol{C}(\eta_k)] \sum_k \{\boldsymbol{\varepsilon}_{tk}\}\bar{\varphi}(\eta_k) \ , \tag{39}$$

$$\bar{\varphi}_k = (\varphi_k/\eta_k, 0) \quad |\eta_k| \geq 0 \ , \tag{40}$$

and the temperature-induced stress coefficient matrix including the phase inhomogeneity

$$[\boldsymbol{C}^\alpha(\eta_k, \alpha_0, \alpha_k)] = [\boldsymbol{C}(\eta_k)]\left([\alpha_0] + \sum_k ([\alpha_k] - [\alpha_0])\varphi(\eta_k)\right) \ , \tag{41}$$

The nonlinear terms are decomposed as

$$G = \sum_k \left(\bar{G}_k + \bar{F}_k\right)\eta_k = \left([\bar{G}] + [\bar{F}]\right)[\boldsymbol{N}_\eta]\{\boldsymbol{v}\}^e = [G']\{\boldsymbol{v}\}^e \ , \tag{42}$$

$$\left\{\frac{\partial G}{\eta_p}\right\} = [\tilde{G}]\{\eta\} = [G'']\{\boldsymbol{v}\}^e \ . \tag{43}$$

In Eq. (35), $\{\boldsymbol{f}\}^e$ is the nodal force vector. In Eq. (36), $\{\boldsymbol{q}_\theta\}^e$ is the thermal flux vector. Considering the effect of ambient environment surrounding the SMA sample, the total thermal flux normal to the material surface (Γ) is defined as $q_\theta = q_0 - h_c(\theta - \theta_0)$, where q_0 is the externally applied flux, θ_0 is the ambient temperature and h_c is the associated convection coefficient.

4 COMPUTATIONAL SCHEME

We implement the finite element model described by Eqs. (35)-(37) with the associated Dirichlet boundary conditions and the initial conditions in a general three-dimensional finite element code. For the present problem we use 8-node, 7 d.o.f/node tetrahedral element with tri-linear isoparametric interpolation and reduced Gauss-quadrature integration for shear terms. Newmark's time integration scheme has been employed, although ensuring the numerical stability for such a strongly coupled problem is not clearly understood at present and require further investigation. In the context of viscoplasticity, the stability issues while using a generalized mid-point rule (first-order accurate) has been discussed in [23]. Extension of such analysis to

a higher-order scheme for the present problem may be needed, since the solid-state transformation process is spontaneous in nature and the associate rates vary substantially compared to continuum elasto-plasticity.

A major complexity arises in the organization of nonlinear iterations. Note that the energy minimization process can take a different and unphysical path unless the phase transformation conditions in Eqs. (8)-(9) are enforced in a consistent manner in the incremental algorithm. Following steps have been adopted:

1. With the known matrices and vectors obtained from the time step $t = t_i$, compute the stress and and transformation barrier.
2. Check the loss of stability $A \leftrightarrow M_k \; \forall k$. Obtain the increment $\Delta\eta_k$ by satisfying consistency condition in the neighborhood of the transformation surface (similar to the return mapping algorithm for elasto-plasticity [23]).
3. Compute the consistent tangent matrix $[\boldsymbol{K}]_t$. Here the effective internal force vector has three parts:
$$\{\boldsymbol{b}\} = \left\{\{\boldsymbol{f}\}_u^T \; \{\boldsymbol{f}\}_\theta^T \; \{\boldsymbol{f}\}_\eta^T\right\}^T \; ,$$
$$\boldsymbol{f}_u = \frac{\partial \Pi_u}{\partial \boldsymbol{u}} \; , \boldsymbol{f}_\theta = \frac{\partial \Pi_\theta}{\partial \theta} \; , \boldsymbol{f}_\eta = \frac{\partial \Pi_{\rm PT}}{\partial \eta_k} \; .$$
The incremental update at nth iteration is obtained as
$$\{\Delta \boldsymbol{v}\}_{n+1}^e = -[\boldsymbol{K}]_t^{-1} \left(\{\boldsymbol{b}\}_{n+1}^{\rm int} - \{\boldsymbol{b}\}_{n+1}^{\rm ext}\right) \; , \tag{44}$$
$$[\boldsymbol{K}]_t = \bigcup_e \frac{\partial \boldsymbol{b}}{\partial \boldsymbol{v}^e} \; ,$$
4. Eq. (44) is then solved by Newton iteration until a specified convergence is achieved.
5. Compute the updated vectors, velocity and acceleration and move to next time step $t_{i+1} = t_i + \Delta t$.

5 NUMERICAL SIMULATION

Here we show a numerical simulation of stress-induced transformation under longitudinal harmonic stress of amplitude $160MPa$ and frequency $5Hz$ applied at one edge of a $100mm \times 50mm \times 100\mu m$ Ni-Al film. The film is assumed to be restrained at the edge $x = 0$. The surfaces are assumed to be in ambient environment ($\theta = 298K$), $\theta_e = 215K$.

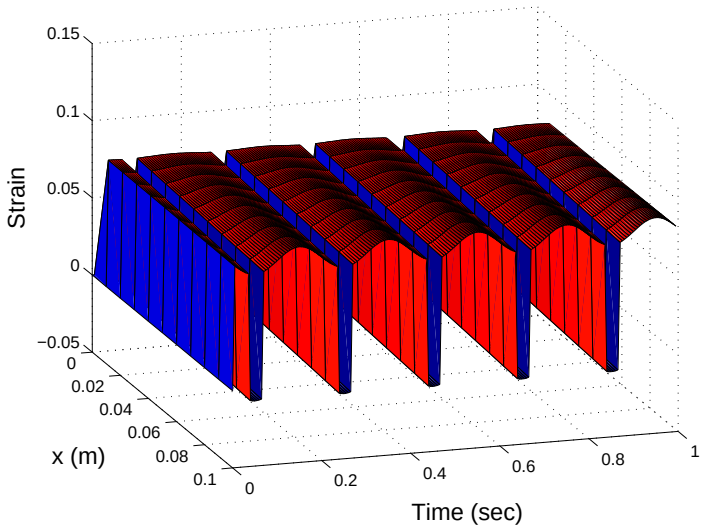

Figure 5. Dynamic strain over the length of the fi lm.

Fig. 5 shows the time history of longitudinal strain ε_{xx} over the length of the film. The transformation induced large strains around the tensile peaks of the loading can be seen, which is with same period as the applied loading. Austenitic wells are formed periodically during stress reversal.

6 CONCLUSIONS

A new Landau-Ginzburg-type free energy model for multivariant martensitic phase transformations has been presented. It is shown that at the onset of transformation, the phase field can be uniquely identified from the conditions of microstructural compatibility. While doing so, the main advantage in the context of solving a discrete version of the energy minimization problem is that the finite element mesh need not be adapted by tracking the A-M_k or M_k-M_j interfaces, instead the order parameters (η_k) can be updated from the equivalent deformation gradient in a point-wise sense. The proposed free energy model follows the essential properties of frame-invariance and material symmetry in 3D situations under thermo-mechanical loading. Based on the developed computational scheme, examplifications have been provided for stress-induced transformations. Such stress-induced transformation dynamics is common in various applications of SMA actuators where the proposed model and the developed computational scheme can be applied in the design optimization.

REFERENCES

[1] J.M. Ball and C. Cartensen, Compatibility conditions for microstructures and the austenite-martensite transition, *Material Science and Engineering A*, 273, 231-236 (1999).

[2] P. Belik and M. Luskin, A computational model for the indentation and phase transition of a martensitic thin film, *J. Mech. Phys. Solids*, 50, 1789-1815 (2002).

[3] M. Brocca, L.C. Brinson and Z.P. Bazant, Three-dimensional constitutive shape memory alloys based on microplane model, *J. Mech. Phys. Solids*, 50, 1051-1077 (2002).

[4] V.I. Levitas and D.L. Preston, Three-dimensional Landau theory for multivariant stress-induced martensitic phase transformations. III. Alternative potentials, critical nuclei, kink solutions, and dislocation theory, *Physical Rev. B*, 68, 134201 (2003).

[5] A. Berezovski and G.A. Maugin, Simulation of wave and front propagation in thermoelastic materials with phase transformation, *Computational Materials Science*, 28, 478-485 (2003).

[6] R.V.N. Melnik, A.J. Roberts and K.A. Thomas, Computing dynamics of copper-based shape memory alloys via center manifold reduction of 3D models, *Computational Materials Science*, 18, 255-268 (2000).

[7] P.K. Purohit and K. Bhattacharya, Dynamics of strings made of phase-transforming materials, *J. Mech. Phys. Solids*, 51, 393-424 (2003).

[8] C. Carstensen, Ten remarks on nonconvex minimization for phase transition simulations, *Comput. Methods. Appl. Mech. Engrg.*, 194, 169-193 (2005).

[9] K. Bhattacharya, *Microstructure of Martensite*, Oxford University Press (2003).

[10] F. Falk and P. Kanopka, Three-dimensional Landau theory describing the martenstic phase transformation of shape -memory alloys, *J. Phys.: Condens. Matter*, 2, 61-77 (1990).

[11] R. Abeyaratne, C. Chu and R.D. James, Kinetics of materials with wiggly energies: The evolution of twinning microstructure in a Cu-Al-Ni shape memory alloys, *Phil. Mag.*, 73A, 457-496 (1996).

[12] A. Artemev, Y. Wang, A.G. Khachaturyan, Three-dimensional phase field model and simulation of martensitic transformation in multilayer systems under applied stresses, *Acta Mater.*, 48, 2503-2518 (2000).

[13] T. Ichitsubo, K. Tanaka, M. Koiwa and Y. Yamazaki, Kinetics of cubic to tetragonal transformation under external field by the time-dependent Ginzburg-Landau approach, *Phy. Rev. B*, 62, 5435 (2000).

[14] V.I. Levitas and D.L. Preston, Three-dimensional Landau theory for multivariant stress-induced martensitic phase transformations. I. Austenite $\leftrightarrow$ martensite, *Physical Rev. B*, 66, 134206 (2002).

[15] V.I. Levitas and D.L. Preston, Three-dimensional Landau theory for multivariant stress-induced martensitic phase transformations. II. Multivariant phase transformations and stress space analysis, *Physical Rev. B*, 66, 134207 (2002).

[16] J.G. Boyd and D.C. Lagoudas, A thermodynamical constitutive constitutive model for shape memory materials. Part I. the monolithic shape memory alloy, *Int. J. Plasticity*, 12(6), 805-842, 1996.

[17] X. Wu, D.S. Grummon, T.J. Pence, Modeling phase fraction shakedown during thermomechanical cycling of shape memory materials, *Materials Science Engineering A*, 273-275, 245-250 (1999).

[18] B. Li and M. Luskin, Finite element analysis of microstructure for the cubic to tetragonal transformation, *SIAM J. Numer. Anal.*, 35, 376-392 (1998).
[19] P. Matus, R.V.N. Melnik, L. Wang and I. Rybak, Application of fully conservative schemes in nonlinear thermoelasticity: modelling shape memory materials, *Mathematics and Computers in Simulation*, 65, 489-510 (2004).
[20] D.R. Mahapatra and R.V.N. Melnik, A dynamic model for phase transformations in 3D samples of shape memory alloys, *LNCS* Springer-Verlag, 3516, 25-32 (2005).
[21] S. Fu, S., Y. Huo, and I. Muller, Thermodynamics of pseudoelasticity - an analytical approach, *Acta Mechanica*, 99, 1-19 (1991).
[22] R.D. James and K.F. Hane, Martensitic transformations and shape memory materials, *Acta Materialia*, 48, 197-222 (2000).
[23] J.C. Simo and T.J.R. Hughes, Computational Inelasticity, Springer-Verlag (1997).

ECCOMAS

II ECCOMAS Thematic Conference on Smart Structures and Materials

Proceedings and Papers

Instituto Superior Técnico, Lisbon 18 / 21 July 2005

Edited by:
Carlos A. Mota Soares, Jan Holnicki-Szulc, Afzal Suleman and Cristóvão M. Mota Soares